5-8-2007

# Optical Properties of Epitaxial Single-Crystal Chemical-Vapor-Deposited Diamond

Giorgio Turri
*University of Central Florida*, turrig@erau.edu

Ying Chen
*University of Central Florida*

Michael Bass
*University of Central Florida*

David Orchard
*QinetiQ Ltd.*

James E. Butler
*Naval Research Observatory*



## Scholarly Commons Citation

Giorgio Turri, Ying Chen, Michael Bass, David Orchard, James E. Butler, Sally Magana, Tatayana Feygelson, Derrick Thiel, Kevin Fourspring, Joni Pentony, Samantha Hawkins, Meghan Baronowski, Randle V. Dewees, Michael D. Seltzer, Andrew Guenthner, Daniel C. Harris, and C. Martin Stickley, "Optical properties of epitaxial single-crystal chemical-vapor-deposited diamond," Proc. SPIE 6545, Window and Dome Technologies and Materials X, 654504 (2007). https://doi.org/10.1117/12.718365

PROCEEDINGS OF SPIE

SPIEDigitalLibrary.org/conference-proceedings-of-spie

# Optical properties of epitaxial single-crystal chemical-vapor-deposited diamond

Giorgio Turri, Ying Chen, Michael Bass, David Orchard, James E. Butler, et al.

Giorgio Turri, Ying Chen, Michael Bass, David Orchard, James E. Butler, Sally Magana, Tatayana Feygelson, Derrick Thiel, Kevin Fourspring, Joni Pentony, Samantha Hawkins, Meghan Baronowski, Randle V. Dewees, Michael D. Seltzer, Andrew Guenthner, Daniel C. Harris, C. Martin Stickley, "Optical properties of epitaxial single-crystal chemical-vapor-deposited diamond," Proc. SPIE 6545, Window and Dome Technologies and Materials X, 654504 (8 May 2007); doi: 10.1117/12.718365

SPIE.

Event: Defense and Security Symposium, 2007, Orlando, Florida, United States

# Optical properties of epitaxial single-crystal chemical-vapor-deposited diamond

Giorgio Turri[1], Ying Chen[1], Michael Bass[1], David Orchard[2], James E. Butler[3], Sally Magana[3], Tatayana Feygelson[3], Derrick Thiel[3], Kevin Fourspring[3], Joni Pentony[4], Samantha Hawkins[4], Meghan Baronowski[4], Randle V. Dewees[4], Michael D. Seltzer[4], Andrew Guenthner[4], Daniel C. Harris[4] and C. Martin Stickley[5]

[1] CREOL, the College of Optics and Photonics, University of Central Florida, Orlando, Florida

[2]QinetiQ Ltd, Malvern, United Kingdom

[3]Naval Research Laboratory, Washington DC

[4]Naval Air Systems Command, China Lake, California

[5]Defense Advanced Research Projects Agency (DARPA), Arlington, Virginia

## ABSTRACT

Epitaxial single-crystal chemical-vapor-deposited diamond was obtained from Element Six Ltd. (Ascot, UK) and from Apollo Diamond (Boston, MA). Both companies provided 5 x 5 mm squares with thicknesses ranging from 0.5 to 1.5 mm. In addition, Element Six provided 10-mm-diameter disks with a thickness of 1.0 mm. The absorptance of all specimens at 1064 nm was measured by laser calorimetry, with good agreement between independent measurements at the University of Central Florida and at QinetiQ (Malvern, UK). Depolarization at 1064 nm and ultraviolet absorption properties are also reported.

Tracking Number : DSS07-DS41-8

**Keywords:** CVD diamond, calorimetry, depolarization loss.

## 1. INTRODUCTION

Diamond has unique properties as an optical material. It combines extreme hardness, chemical inertness, high thermal conductivity and a broad band transparency, typically extending from the far infrared to the near ultraviolet[1,2,3,4]. Large area diamond windows and hemispherical domes with properties similar to, or better than, those of the best type IIa natural single-crystal diamond, can be grown in relatively short times by chemical-vapor-deposition (CVD)[5,6]. CVD diamond windows find applications in industrial and military environments, including high power lasers, IR imaging systems, gyrotron tubes and heat-seeking missiles[7,8].

This study assesses optical properties of state-of-the-art epitaxially grown CVD single-crystal diamond at a wavelength of 1.064 μm for potential application as a heat spreading element in solid state lasers. Laser calorimetry was used to measure the absorptance (fraction of incident irradiation that is absorbed) in different specimens. In this technique, the change in temperature of a specimen is measured as a function of time when the specimen is exposed to a known laser

Window and Dome Technologies and Materials X, edited by Randal W. Tustison,
Proc. of SPIE Vol. 6545, 654504, (2007)
0277-786X/07/$18 · doi: 10.1117/12.718365

power and after the exposure is ended[9,10]. Laser calorimetry has the advantages of the simplicity of the apparatus and ease of absolute calibration, and for these reasons it is the recommended method for characterizing laser optical components[11]. It also allows for laterally resolved measurements, though with less precision than other techniques, such as photothermal deflection[9], but it does not distinguish between absorption in the bulk and absorption due to impurities and defects on the specimen surfaces. In order to disentangle these two contributions, we measured the absorptance in specimens with different thicknesses and supposedly identical surfaces. Then a plot of measured absorptance versus specimen thickness extrapolated to zero thickness should reveal the surface absorptance and the slope of the graph should give the bulk absorptance. The loss of polarization of light crossing the specimen was also measured, using the well-known optical technique of placing the investigated specimen between two polarizers and measuring the light transmitted for different specimen and polarizers orientations. Finally, the ultraviolet absorption edge of the specimens was investigated using a Cary 500 spectrophotomer. A complete report of this work is in press[12].

The diamonds used for this investigation were manufactured in 2005 by Element Six (Ascot, UK) and Apollo Diamond (Boston, MA). Both companies supplied diamond squares with nominal dimensions of 5 x 5 mm and thickness in the range 0.35–1.75 mm. In addition, Element Six provided disks with a state-of-the-art diameter of 10–11 mm and a thickness of 1.0 mm. Table 1 depicts the size and thickness of the investigated specimens.

**Table 1.** Diamond size and thickness.

| Specimen | Thickness [mm] | Specimen | Thickness [mm] |
|---|---|---|---|
| ***Squares with nominal dimensions of 5 x 5 mm*** | | | |
| Element Six #1 | 0.43 | Apollo #1 | 0.35 |
| Element Six #2 | 0.50 | Apollo #2 | 0.68 |
| Element Six #3 | 0.92 | Apollo #3 | 1.09 |
| Element Six #4 | 1.00 | Apollo #4 | 1.74 |
| Element Six #5 | 1.42 | Apollo #5 | 0.35 |
| Element Six #6 | 1.47 | | |
| ***Disks with diameter 10–11 mm (by ElementSix)*** | | | |
| Disk 1 | 1.03 | | |
| Disk 2 | 1.07 | | |
| Disk 3 | 1.03 | Apollo #6* | 1.27 |

*Apollo #6 is a 3.6-mm-diameter disk

Apollo #4 appears dark grey, and Element Six Disks 1,2,3 slightly grey, to the eye while all the other specimens are colorless. Apollo #6 is supposed to be the state-of-the-art optical quality product of Apollo, whereas Apollo #1 to #5 are expected to be of somewhat lower quality. (Apollo, private communication).

The 5 x 5 mm squares obtained from Element Six were commercially available at a cost of ~$100 US per cubic millimeter in 2005. Disks from Element Six and squares from Apollo were larger than what either company has produced in the past and therefore were not commercially priced. In the following, the investigated specimens will be labeled accordingly to Table 1.

## 2. EXPERIMENTAL

### 2.1 Laser calorimetry

Laser calorimetry was conducted at CREOL, The College of Optics and Photonics at the University of Central Florida, and, independently, at QinetiQ (Malvern, UK). At CREOL, a recently built calorimeter was employed, consisting of a styrofoam box, at ambient temperature in the air, enclosing the experiment to provide thermal isolation of the specimen. The specimen was held by a piece of a monofilament fishing line glued to its edge and attached to a thermally isolated frame with three degrees of translational and rotational movement. A Precision Temperature Measurement System by GEC Instruments (model S4TC) allowed the simultaneous reading of up to four temperatures with precision better than 10 mK over a broad range. Three 0.2-mm-diameter thermocouples were glued to the specimen, whereas the forth thermocouple was used to record a benchmark signal synchronized with the start and the stop of the specimen irradiation. Care was taken to prevent scattered laser light from striking the temperature sensors. Laser light entered and exited the calorimeter through holes in which plastic tubes were inserted to reduce convective heat transfer. A continuous wave laser, emitting at 1.064 μm in $TEM_{00}$ mode, with power between 0.1 and 3 W, was focused to ~ 1 mm diameter on the entrance surface of the specimen. The overall sensitivity of the calorimeter was about 10 mK.

Examples of the irradiation-induced temperature change vs. time are shown in Figure 1. For each specimen and location, ten or more plots were made with irradiation times ranging from 100 to 200 s, and the results averaged. Two independent methods were employed to extract the absorptance from the observed temperature vs. time plots. If the thermal conductivity of the specimen is high enough that its temperature (T) is uniform as is the case for diamond, the temperature variation from the ambient temperature (ΔT) vs. time (t) is given by[9]:

During irradiation:
$$\Delta T = \frac{aP}{\gamma m c_p}\left[1 - e^{-\gamma(t - t_{start})}\right] \quad (1)$$

After irradiation
$$\Delta T = \frac{aP}{\gamma m c_p}\left[e^{-\gamma(t - t_{stop})} - e^{-\gamma(t - t_{start})}\right] \quad (2)$$

where a is the absorptance, m is the mass of the specimen, P is the incident laser power, $c_p$ is the heat capacity (for diamond $c_p$ =0.51 J/(g*K))[13,14,15], γ is a heat loss coefficient, $t_{start}$ is the time at which the specimen is exposed to the laser and $t_{stop}$ is the time at which exposure is ended. Then, the absorptance can be obtained by fitting the measured data using Eqns. (1) and (2) with a and γ as free parameters. In the following we shall refer to this technique as the "fit method". The second technique employed to analyze the CREOL data, is known as the "gradient method"[9]. It consists of taking the derivative with respect to time of the irradiation-induced temperature change versus time at two instants $t_h$ and $t_c$, during irradiation and after irradiation. For the gradient method, $t_h$ and $t_c$ are chosen so that the temperature at each instant is the same. From the derivatives taken at these two times the absorptance is obtained from

$$\frac{d}{dt}\Delta T(t_h) - \frac{d}{dt}\Delta T(t_c) = \frac{a\,P}{m c_p} \quad (3)$$

The fit and gradient methods gave similar results, typically disagreeing by less than 5%.

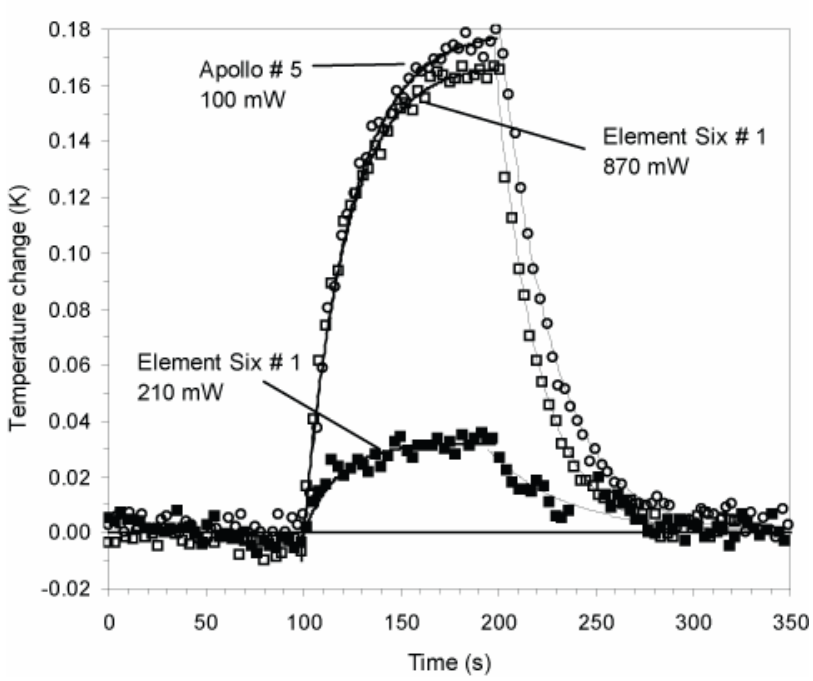


**Fig. 1.** Irradiation-induced temperature change vs. time for Apollo #5 (350 μm thick) and Element Six #1 (430 μm thick) with irradiation time of 100 s. Lines are independent fits to the heating and cooling data with Eqns. (1) and (2). (CREOL data.)

At QinetiQ, calorimetry was performed in a similar manner with specimens at 300 K in the air. The specimen was held by a network of nylon filaments which grip the specimen around its edge. Specimen temperature was measured by a thermocouple held in contact with the specimen edge by one of the filaments. The diode-pumped Nd:YAG laser operated at 1.064 μm with a power of 250 mW and the beam at the specimen had dimensions of ~0.15 x 0.34 mm. The method used to extract absorptance from calorimetry data at QinetiQ has been described previously[10]. Briefly, the heat loss coefficient $\gamma$ and ambient temperature were obtained by fitting the cooling curve. With these values of $\gamma$ and ambient temperature, the heating curve was fit by using a point-by-point graphical procedure to find absorptance.

The absorptance a is related to the absorption coefficient $\alpha$ defined by the equation

$$\text{Internal transmittance} = e^{-\alpha l} \tag{4}$$

Internal transmittance is the fraction of radiant power that has entered a specimen that reaches the opposite side after traversing a pathlength l through the specimen. Internal transmittance is independent of surface losses by reflection, absorption, and scattering. For perpendicular incidence of the laser beam on a specimen with parallel surfaces, negligible scattering, and negligible surface absorption, the relation between a and $\alpha$ is:

$$e^{-\alpha l} = \frac{\tau - a}{\tau - Ra} \tag{5}$$

where $\tau$ is the transmittance of the specimen and R is the single-surface Fresnel reflectance. When $\alpha l \ll 1$, a first-order expansion of Eq. (5) gives:

$$a \approx \alpha l \tag{6}$$

If there is surface absorption, a term accounting for both surfaces is added to Eq. (6) so that

$$a \approx \alpha l + \alpha_{surface} \tag{7}$$

For our specimens, ($\alpha$) ranged between $10^{-2}$ and $10^{-3}$ $cm^{-1}$ and $l \approx 10^{-1}$ cm, so Eq. (6) and (7) apply.

### 2.2 Loss of polarization

The apparatus in Figure 2 was used at CREOL to measure loss of polarization of plane-polarized 1.064 μm radiation from a Nd:$YVO_4$ laser. A 3-mm-diameter aperture limited the area of the diamond tested. When no specimen was placed in front of the aperture, no measurable power was detected if the analyzer polarizer was set to transmit light polarized perpendicular to the laser polarization, whereas transmission through the analyzer was 0.887 if this was set to transmit light polarized in the same plane as the laser. Before making a measurement, the center of the diamond/aperture combination was aligned with the axis of the laser beam and the analyzer polarized was removed. The diamond/aperture combination was then rotated about the beam axis to see if transmission changed. Less than 1.0 % variation was observed for all the square specimens however the disks showed significant changes in transmission, as discussed in section 3.

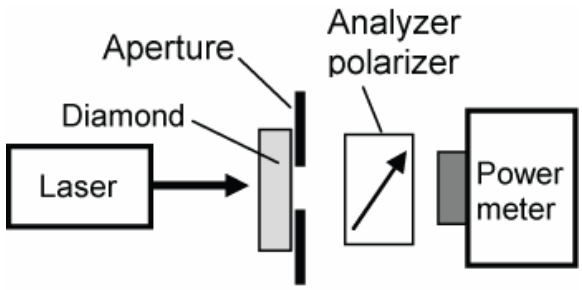


**Fig. 2.** Schematic diagram of the experiment for measuring loss of polarization. A linearly polarized Nd:$YVO_4$ diode-pumped laser was the source in this experiment.

When the analyzer polarizer was inserted and aligned to transmit light polarized parallel to the laser's polarization, the transmitted power $P_t$ should be $P_d$*0.887 if there were no depolarization loss. The observed transmitted power was less than $P_d$*0.887 and varied as the diamond was rotated about the beam axis. For each specimen orientation, the observed transmitted power was expressed as a percent of theoretical transmitted power in the absence of depolarization according to the formula:

$$\%T = 100 \times \frac{P_t}{Pd * 0.887} \tag{8}$$

With this technique, the transmission losses due to the reflection from the surfaces of the specimen and of the analyzer polarizer were properly taken into account.

### 2.3 Ultraviolet-edge absorption

Measurements were performed at CREOL using a Cary 500 dual-beam spectrophotometer operated with unpolarized light. The specimen transmittance was measured at 1 nm intervals in the 0.2 to 2 μm range while the instrument's spectral bandwidth was fixed at 4 nm. Reflections from the front and back surfaces of the specimen were accounted for by using the Fresnel formula, the refractive index values available in literature and the Peter's trend for dispersion in diamond [16,17]. A further correction was necessary to account for changes in the measured transmission due to experimental errors, either introduced by the specimen (e.g., non-perfect parallelism of the surfaces and light scattering inside the specimen) or by the spectrophotometer (e.g., wavelength-dependent efficiency). These effects are typical of the spectrophotometry technique and they may cause either an over- or an under-estimation of the zero in the measured absorption spectrum. In this paper, we estimate the effects of these errors to be +/- 10% of the reflections at the surfaces calculated using the Fresnel formula. Independent spectrophotometric measurements of all the specimens, similar to the above described ones, were performed at the Naval Air Systems Command, China Lake, CA.

## 3. RESULTS

### 3.1 Absorption at 1.064 μm.

Columns 3 and 4 of table 2, depict the results of the absorptance measurements from CREOL and QuinetiQ: each value is an average of measurements at 3 to 8 locations. Data from CREOL and QinetiQ are in reasonable agreement. All specimens showed significant point-to-point variation in the absorption. The deviations from the average reported in Table 2 between different locations on the same specimen were in the range of 5 to 46%.

Absorptance versus specimen thickness for the diamond squares is plotted in Figure 3. Ideally, the points should lie on a straight line with an intercept of 0 (Eq. 6) if there is no surface absorption or $\alpha_{surface}$ (Eq. 7) if there is surface absorption. For Element Six squares, the absorptance of specimens l, 2, 4, 5, and 6 lies near a straight line in Figure 3. The higher absorptance of specimen 3 is clearly not from the same population. The slope of the line for Element Six in Figure 3 gives an absorption coefficient of $\alpha = 0.0026 \pm 0.0005$ cm$^{-1}$. The intercept of $0.006 \pm 0.006$ implies that there is little surface absorptance. For Apollo material, a line in Figure 3 was fit to specimens 3 and 5, plus one measurement for specimen 2. Apollo #4, which is not shown on the graph, had much higher absorptance and was clearly not in the same population. Apollo #6, which is shown on the graph, has much lower absorptance than the other specimens. The slope of the line for Apollo material in Figure 3 gives an absorption coefficient of $\alpha = 0.071 \pm 0.005$ cm$^{-1}$ and the intercept is $- 0.13 \pm 0.04$. Since surface absorptance cannot be negative, we attribute the negative intercept to variability of the absorptance in the small number of specimens.

Neglecting possible contribution from surface absorption, the mean absorption coefficient of Element Six disks is 0.008 cm$^{-1}$ for Disk 1, and 0.03 cm$^{-1}$ for Disks 2 and 3. These absorption coefficients are 3–10 times greater than that of Element Six squares and comparable with those of Apollo #2, #3 and #5. The high quality specimen from Apollo has an absorption coefficient comparable with those of Element Six squares.

Very few absorption measurements in diamond are available in the literature, and most of them have been performed at 10.6 μm, where high-order phonons processes produce a weak absorption band[18]. To the best of our knowledge, the only published measurements around 1 μm are Mollart's et al.[19] and Godfried's et al[6]. The absorption coefficients we measured in Apollo #6 and Element Six squares, are one order of magnitude lower than reported in Ref. 19 and a factor 2 to 4 lower less than reported in Ref. 6.

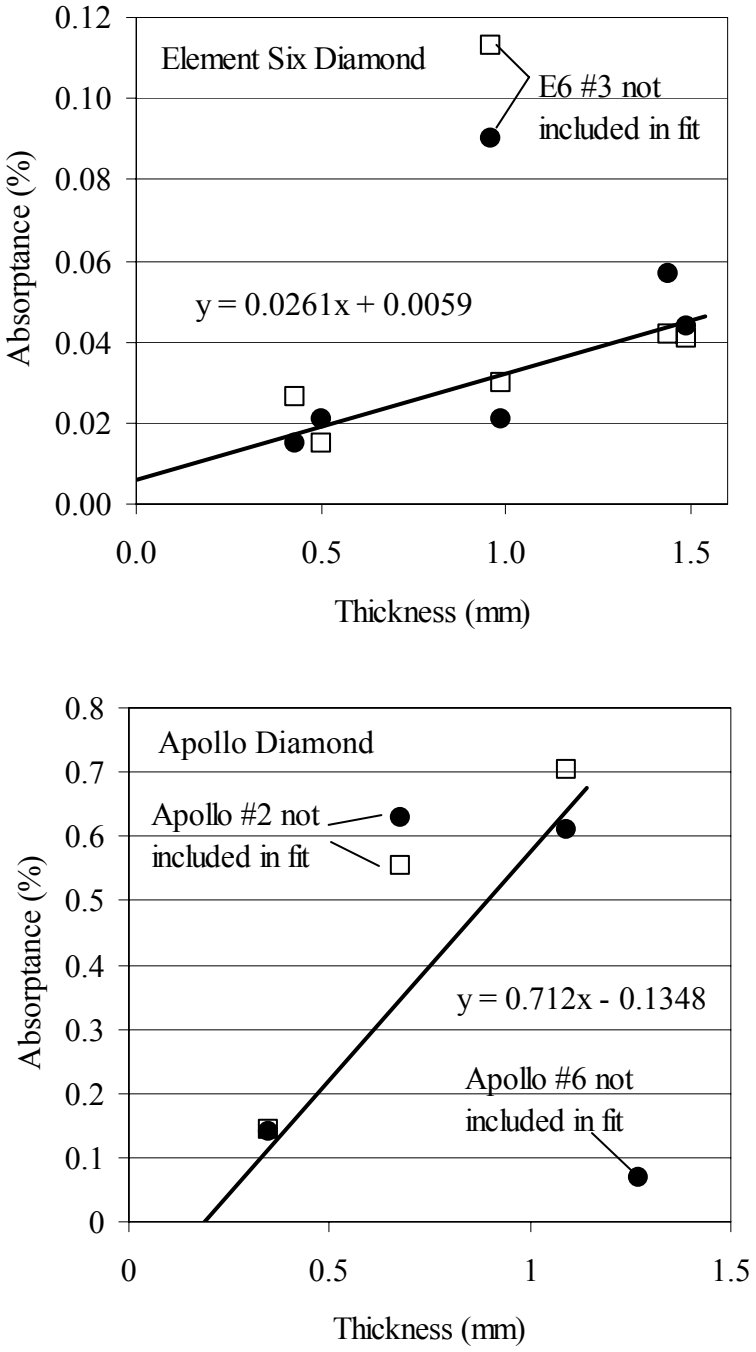


**Fig. 3.** Absorptance of diamond at 1.064 μm as a function of thickness for Element Six (top panel) and Apollo diamond squares (bottom panel). Circles: CREOL measurements; squares: QinetiQ measurements.

### 3.2 Loss of polarization at 1.064 μm.

Different degrees of depolarization were observed as each specimen was rotated about the axis of the laser beam. Columns 4 and 5 of Table 2 show the minimum and maximum loss of polarization observed for each specimen. The angular separation between minimum and maximum was not 90º. Most square specimens had an orientation in which the loss of polarization was less than 5%.

The measurement of depolarization of the disks from Element Six was more difficult. The transmittance of these specimens was observed to depend on their orientation with respect to the polarization of the laser light. Transmittance varied by 20% in Disk 1, 5% in Disk 3, and less than 1% in Disk 2 as the specimen was rotated. This variation makes it difficult to disentangle the loss of transmission from the loss of polarization induced by the specimen, when using the apparatus in Figure 3. By comparing measurements with and without the analyzer polarizer for the same rotation angle of the Disks, we could conclude that the loss of transmission is larger than the loss of polarization for Disks 2 and 3.

**Table 2.** Calorimetric absorptance and loss of polarization, at 1.064 μm

| Specimen* | Thickness (mm) | Calorimetric absorptance (%) CREOL | QinetiQ | Loss of polarization (%) Minimum† | Maximum† |
|---|---|---|---|---|---|
| ***Squares with nominal dimensions of 5 x 5 mm*** | | | | | |
| Element 6 #1 | 0.43 | 0.015 | 0.026 | 3.6 | 22.4 |
| Element 6 #2 | 0.50 | 0.021 | 0.015 | 4.1 | 17.9 |
| Element 6 #3 | 0.92 | 0.090 | 0.113 | 8.3 | 26.5 |
| Element 6 #4 | 1.00 | 0.021 | 0.039 | 2.6 | 9.5 |
| Element 6 #5 | 1.42 | 0.057 | 0.042 | 9.4 | 21.7 |
| Element 6 #6 | 1.47 | 0.044 | 0.041 | 5.1 | 17.5 |
| Apollo #1 | 0.35 | --- | --- | --- | --- |
| Apollo #2 | 0.68 | 0.63 | 0.55 | 2.3 | 11.7 |
| Apollo #3 | 1.09 | 0.61 | 0.70 | 3.6 | 15.4 |
| Apollo #4 | 1.74 | 7.2 | --- | 11.1 | 21.0 |
| Apollo #5 | 0.35 | 0.14 | 0.14 | 1.3 | 11.7 |
| Apollo #6* | 1.27 | 0.069 | --- | 0.0 | 8.2 |
| ***Disks with diameter 10–11 mm*** | | | | | |
| Element 6 disk 1 | 1.03 | 0.085 | 0.075 | 1 | 4 |
| Element 6 disk 2 | 1.07 | 0.32 | 0.36 | 0 | 4 |
| Element 6 disk 3 | 1.03 | 0.25 | 0.28 | 0 | 3 |

*Apollo #6 is a 3.6-mm-diameter disk

†Transmittance calculated with Eq. (8)

### 3.3 Ultraviolet edge.

The two panels of Figure 4 depict the absorbance, defined as the logarithm to the base 10 of the ratio between the incident and the transmitted power for Apollo and Element Six specimens in the near-ultraviolet region. The absorbance of Element Six specimens for wavelength longer than 236 nm is near the theoretical reflection limit, shown by the dashed line computed from the Fresnel reflection. Apollo #1, #2, #3, and #5 exhibit barely detectable absorption in the region 240-300 nm, whereas Apollo #4, which has a strong absorption at 1.064 μm, has also stronger ultraviolet absorption than all other specimens. The value of the absorbance measured at 1.064 μm for Apollo #4 (not shown in Figure 4) is consistent with the value of the absorptance obtained at that wavelength by calorimetry; for all the other specimens the absorbance measured around 1 μm is too low to allow a similar comparison with the calorimetric measurements.

Diamond is an indirect-gap semiconductor with first conduction band energy gap of 5.49 eV corresponding to a transition around 226 nm [20] (e.g., its ultraviolet edge). Since this is an indirect transition, i.e. the electron has a different momentum in the conduction band than it did in the valence band, the excitation of the first conduction band can occur only with the participation of phonons. At room temperature, one photon absorption occurs with highest probability in association with the absorption of one transverse optic, one transverse acoustic or the emission of one transverse acoustic phonon. The three processes have thresholds around 236, 234 and 225 nm respectively, the latter being associated with the most intense absorption cross section[21,22].

In addition to this "intrinsic" absorption, lattice defects and impurities cause an "extrinsic" absorption which both increases the absorption coefficient on the ultraviolet edge and extends it to wavelengths longer than 236 nm. By means of absorption measurements at different temperatures, Clark[22] was able to separate extrinsic from intrinsic contributions in the absorption spectrum of real diamond, and the absorption coefficients of the intrinsic absorption around the ultraviolet edge are now known[20,22]. The intrinsic absorption coefficients of diamond are compared to the values measured at CREOL and at the Naval Air Systems Command in Figure 5, where the average of all the square Element Six specimens and of Apollo 2, 3, 5 and 6 is reported. No evidence of extrinsic contribution to the absorption is observable.

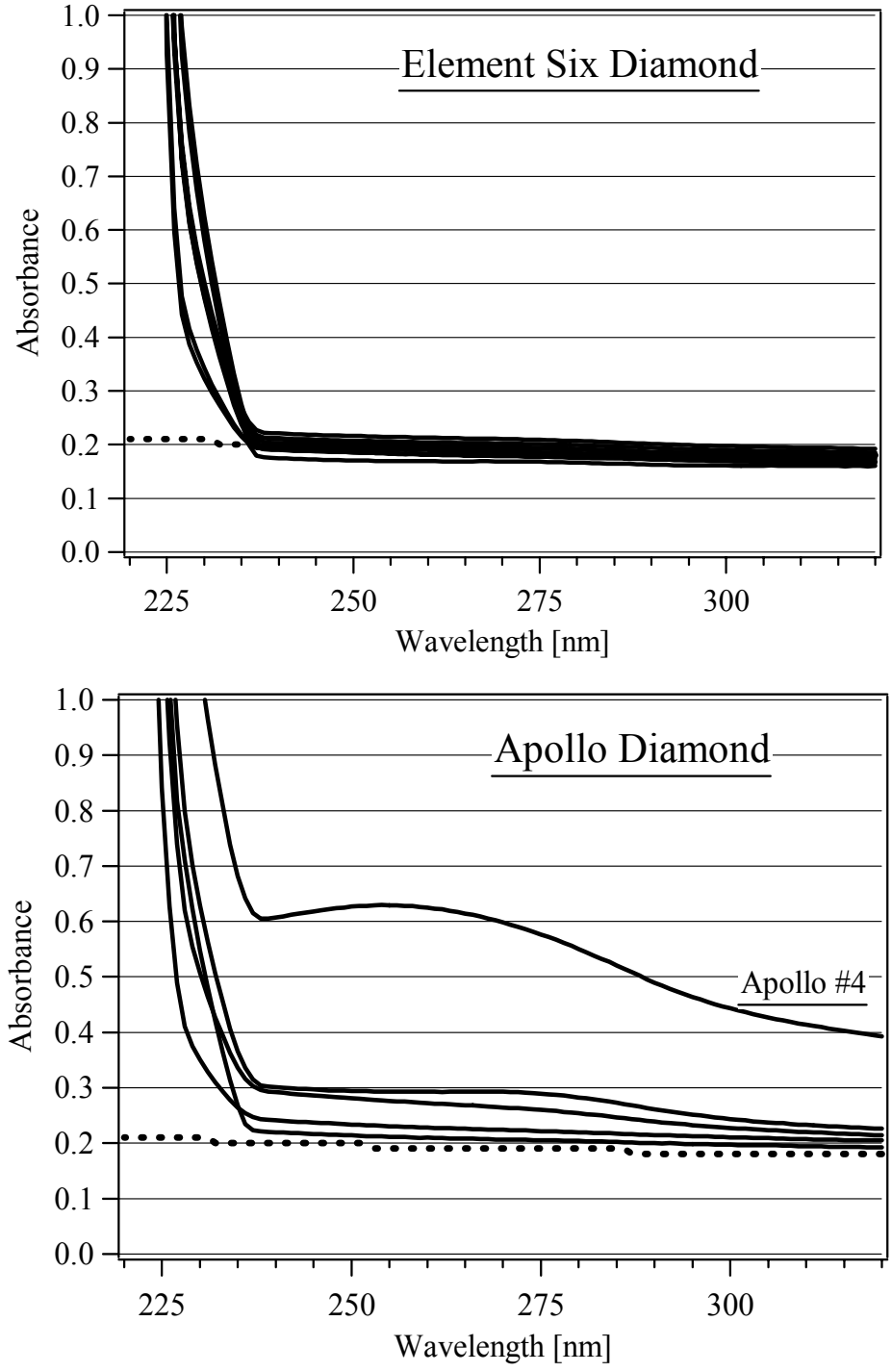


**Fig. 4.** Ultraviolet absorption of nine Element Six specimens (top panel) and 4 Apollo specimens (bottom panel). The theoretical reflection limit is shown by the dashed line computed for Fresnel reflection based on the reported indices of refraction.

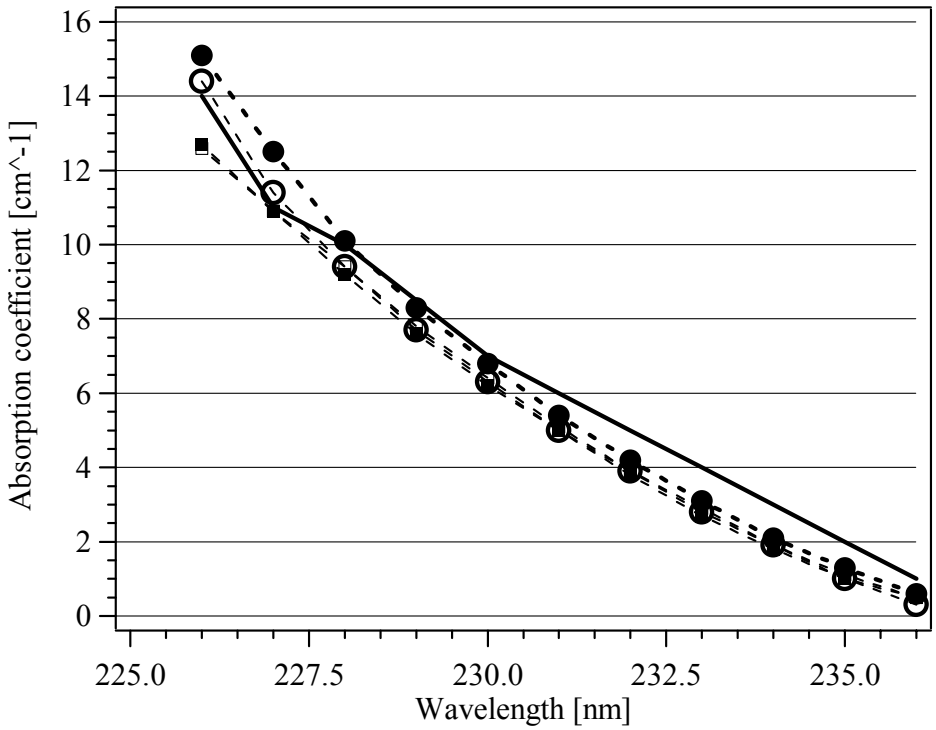


**Fig. 5.** Absorption coefficient at different wavelength near the ultraviolet absorption edge. Average of Element Six squares : ○ CREOL, □ Naval Air Systems Command. Average of Apollo #1, #2, #3 and #5 : ● CREOL, ■ Naval Air Systems Command. ━ Intrinsic absorption[20,22].

## 4. CONCLUSIONS

The purpose of the present study was to evaluate optical properties of single-crystal epitaxial CVD diamond at 1.064 μm relevant to its use as a heat spreading element in the optical path of a solid state laser. The absorption coefficient of diamond from Element Six was approximately 0.003 $cm^{-1}$. Diamond elements with a total thickness of 1 cm in the optical path of a 1.064 μm laser would absorb only 0.3% of the energy of the beam. This is the lowest absorption ever measured in either natural or synthetic diamond. For Apollo material examined in this study, the absorption would be 7%, but there was one Apollo specimen whose absorption was only twice as great as that of Element Six material. It should also be noted that both manufacturers obtained the highest optical quality in the smallest size specimens.

Loss of polarization by radiation traversing the solid state laser is a serious issue. We observed varying loss of polarization as diamond squares were rotated about their <100> axis parallel to the path of the laser beam. Table 2 shows that, for most squares from Element Six or from Apollo, there was an orientation in which the loss of polarization was <5%. Disks from Element 6 had an optimum orientation in which their loss of polarization was <1%. Even in their worst orientation, loss of polarization from the disks was less than loss from the squares. Our results are qualitatively similar to the range of birefringence observed by van Loon et al[23].

Absorption and loss of polarization are sufficiently low for selected, properly oriented specimens of single-crystal, epitaxial CVD diamond to be used as a heat spreading element in the optical path of a solid state laser.

**Acknowledgement**

This work was supported by the Defense Advanced Research Projects Agency Microsystems Technology Office.

## REFERENCES

1. G. Davies, "The Optical Properties of Diamond" in *Chemistry and Physics of Carbon* Vol. 13 (P. L. Walker, Jr. and P. A. Thrower, Eds.) Marcel Dekker, New York, 1977.
2. J. Field, Ed., *The Properties of Natural and Synthetic Diamond*, Academic Press, London, 1992.
3. G. Davies, Ed., *Properties and Growth of Diamond*, INSPEC, London, 1994.
4. J. Wilks and E. Wilks, *Properties and Applications of Diamond*, Butterworth Heinemann, Oxford, 1991.
5. M. Werner and R. Locher, "Growth and application of undoped and doped diamond films", *Rep. Prog. Phys.*, **61**, 1665-1710, 1998.
6. H.P. Godfried, G.A. Scarsbrook, D.J. Twitchen, E. Houwman, W.G.M. Nelissen, A.J. Whitehead, C.E. Hall, and P.M. Martineau, "Optical Quality Diamond Material," European Patent GB2411895 (14 Sep 2005); U.S. Patent Application 2004/0229464.
7. T.P. Mollart, K.L. Lewis, C.S.J. Pickles and C.J.H. Wort, "Factors affecting the optical performance of CVD diamond infrared optics", *Semicond. Sci. Technol.*, **18**, S117-S124, 2003 and references therein.
8. C.S.J. Pickles, T.D. Madgwick, R.S. Sussmann and C.J.H. Wort, "Optical performance of chemically vapour-deposited diamond at infrared wavelengths", *Diam. Relat. Mater.*, **9**, 916-920, 2000.
9. U.Willamowski, D.Ristau and E..Welsch, "Measuring the Absolute Absorptance of Optical Laser Components," *Appl. Opt*., **37**, 8362-8370, 1998.
10. D.A. Orchard, P.D. Mason, E.J. McBrearty and K. L. Lewis, "Laser Calorimetry as a Tool for the Optimisation of MidIR OPO Materials", *Proc SPIE* **5273**, 379-387, 2003.
11. "Test method for Absorptance of Optical Laser Components" ISO/FDIS 11551 (International Organization for Standardization, Geneva, 1995).
12. G. Turri, Y. Chen, M. Bass, D. Orchard, J. E. Butler, S. Magana, T. Feygelson, D. Thiel, K. Fourspring, R. V. Dewees, J. M. Bennett, J. Pentony S. Hawkins, M. Baronowski, A. Guenthner, M. D. Seltzer, D. C. Harris and C. M. Stickley, "Optical Absorption, Depolarization, and Scatter of Epitaxial, Single-Crystal Chemical-Vapor-Deposited Diamond at 1.064 μm," *Opt. Eng.*, 2007, in press.
13. A. C. Victor, "Heat Capacity of Diamond at High Temperature," *J. Chem. Phys*., **36**, 1903-1911, 1962.
14. D. L. Burk and S. A. Frieberg, "Atomic Heat of Diamond from 11° to 200°K," *Phys. Rev*., **111**, 1275-1282, 1958.
15. J. E. Graebner, "Measurements of Specific Heat and Mass Density in CVD Diamond," *Diamond Relat. Mater*. **5**, 1366-1370, 1996.
16. D.F. Edwards and E. Ochoa, "Infrared refractive index of diamond", *J. Opt. Soc. Am.*, **71**, 607-608, 1981.
17. F. Peter, "Uber Brechungsindizes und Absoptionskonstanten des diamanten zwischen 644 und 226 mμ", *Z. Phys.*, **15**, 358-368, 1923 (in German).
18. Z. Remes, M. Nesladek and C.S.J. Pickles, "Local variations in temperature dependence of optical absorption coefficient in natural IIa type and CVD diamond optical windows", *Phys. Stat. Sol. (a)*, **186**, 297-301, 2001.
19. T.P. Mollart, K.L. Lewis, C.S.J. Pickles and C.J.H. Wort, "Factors affecting the optical performance of CVD diamond infrared optics", *Semicond. Sci. Technol.*, **18**, S117-S214, 2003.
20. A.T. Collins, "Intrinsic and extrinsic absorption and luminescence in diamond", *Physica B*, **185**, 284-296, 1993.
21. M.E. Thomas, W.J. Tropf and A. Szpak, "Optical properties of diamond", *Diamond Films and Technology*, **5**, 159-180, 1995.
22. C.D. Clark, "The absorption edge spectrum of diamond", *J. Phys. Chem. Solids*, **8**, 481-485, 1958
23. F. van Loon, A. J. Kemp, A. J. Maclean, S. Calvez, J.-M. Hopkins, J. E. Hastie, M. D. Dawson, and D. Burns, "Intracavity Diamond Heatspreaders in Lasers: The Effects of Birefringence," *Optics Express*, **14**, 9250-9260, 2006.